D2.3. Requirement list for the TRL4 Flexby system

FLEXBY

FLEXIBLE AND ADVANCED BIOFUEL TECHNOLOGY THROUGH AN INNOVATIVE MICROWAVE PYROLYSIS & HYDROGEN-FREE HYDRODEOXYGENATION PROCESS

Grant Agreement Number 101144144

Deliverable name:	Requirement list for the TRL4 Flexby system
Deliverable number:	2.3
Deliverable type:	Report
Work Package:	WP2: FLEXBY requirements
Lead beneficiary:	PMI
Contact person:	Flavio Manenti / flavio.manenti@polimi.it
Dissemination Level:	Public
Due date for deliverable:	February 28, 2025

Funded by
the European Union

DOCUMENT CONTROL PAGE

Author(s):	Flavio Manenti
Contributor(s):	Marcello Maria Bozzini
Reviewer(s):	Nuria Ferrera Lorenzo
Version number:	v.1
Contractual delivery date:	28-02-2025
Actual delivery date:	[dd-mm-yyyy]
Status:	Draft

REVISION HISTORY

Version	Date	Author/Reviewer	Notes
v.0	27-01-2025	Marcello Bozzini	Creation
v.1	10-02-2025	Flavio Manenti	Ready for review
v.2	13-02-2025	IDENER	First version revised
v.3	18-02-2025	PMI	Ready for review
v.4	19-02-2025	IDENER	Final version revised
v.5	26-02-2025	PMI	Ready for submission

ACKNOWLEDGEMENTS

The work described in this publication was subsidised by Horizon Europe (HORIZON) framework through the Grant Agreement Number 101144144.

DISCLAIMER

TABLE OF CONTENTS

DOCUMENT CONTROL PAGE 2

REVISION HISTORY 2

ACKNOWLEDGEMENTS 2

DISCLAIMER 2

TABLE OF CONTENTS 3

TABLE INDEX 4

FIGURE INDEX 4

EXECUTIVE SUMMARY 6

1. INTRODUCTION 7

1.1 DESCRIPTION OF THE DOCUMENT AND PURSUE 7

1.2 WPS AND TASKS RELATED WITH THE DELIVERABLE 7

2. Coordination Among Project Partners and General Requirements 9

3. State-of-the-Art review 12

4. Initial requirements for basic engineering design 14

4.1 Block Flow Diagram and required process units 16

5. Simulation and techno-feasibility analysis of the process 19

5.1 Process Flow Diagram of Flexby process 19

6. Datasheet, energy and mass balances 25

6.1 Algae residue feedstock (Feedstock 2) 26

6.2 Oily-sludge feedstock (Feedstock 6) 30

6.3 Comparison between Feedstock 2 and Feedstock 6 and critical parameters definition 33

7. Conclusions.. 35

8. REFERENCES.. 36

TABLE INDEX

Table 4.1: Flexby unit operation's temperatures and pressures…………………………15

Table 4.2: Proximate and Ultimate analysis of the feedstocks……………………………15

Table 5.1: Input parameters for Aspen Plus simulation……………………..…………20

Table 5.2: Input parameters for pyrolysis gas post-processing Aspen HYSYS Simulation………………………………………………………………………………..23

Table 5.3: Input parameters for bio-liquid refining Aspen HYSYS simulation………….25

Table 6.1: Products of the microwave pyrolysis of Feedstock 2…………………………26

Table 6.2: Pyrolysis gas post-processing datasheet (see Figure 5.4 for stream numbers, Feedstock 2)……………………………………………………………………………..26

Table 6.3: Bio-liquid refining datasheet (see Figure 5.6 for stream numbers, Feedstock 2)……………………………………………………………………………..28

Table 6.4: Energy streams of the process (see Figures 5.4 and 5.6 for stream numbers, Feedstock 2)……………………………………………………………………………..29

Table 6.5: Products of the microwave pyrolysis of Feedstock 6…………………………30

Table 6.6: Pyrolysis gas post-processing datasheet (see Figure 5.4 for stream numbers, Feedstock 6)……………………………………………………………………………..30

Table 6.7: Bio-liquid refining datasheet (see Figure 5.6 for stream numbers, Feedstock 6)……………………………………………………………………………..32

Table 6.8: Energy streams of the process (see Figures 5.4 and 5.6 for stream numbers, Feedstock 6)……………………………………………………………………………..23

FIGURE INDEX

Figure 4.1: Process Flow Diagram of the Flexby process………………………………17

Figure 4.2: Pre-design of the Microwave Pyrolysis Reactor……………………..….......18

Figure 5.1: Simulation of the MW pyrolysis reactor in Aspen Plus V14…………………20

Figure 5.2: First section of the pyrolysis gas post-processing simulation in Aspen HYSYS V14………………………………………………………………………………21

Figure 5.3: Second section of the pyrolysis gas post-processing simulation in Aspen HYSYS V14……………………………………………………………………………………21
Figure 5.4: Process Flow Diagram (PFD) of pyrolysis gas post-processing……………22
Figure 5.5: Bio-liquid post-processing simulation in Aspen HYSYS V14……………….24
Figure 5.6: Process Flow Diagram of bio-liquid refining………………………………….24

EXECUTIVE SUMMARY

This document corresponds to the technical report “Requirement List for the TRL4 Flexby System” (Deliverable 2.3). It presents the study conducted by **PMI**, with the support of the consortium partners, to define the initial requirements for the FLEXBY system and establish the basis for the process's basic engineering. The report includes steady-state process simulations, heat and mass balances, and a comparison between different feedstocks. It serves as a foundation for lab-scale experimental tests and the subsequent pilot-scale implementation.

To begin with, several meetings were held with each consortium partner to address the process's initial requirements and key challenges. The availability of feedstock was assessed in relation to the lab-scale experimental tests at **CSIC** and **US**, ensuring alignment with **FRIMA**'s specifications for constructing the microwave pyrolysis reactor. Additionally, **GD** and **IDE** outlined their needs regarding the LCA assessment and process optimization, respectively.

Following this, **PMI** conducted a comprehensive State-of-the-Art review of the technological solutions applied in the process, defining operating conditions and identifying key critical parameters. In parallel, a Block Flow Diagram (BFD) of the process was developed as an initial step before carrying out process simulations.

Finally, two steady-state process simulations were performed using **Feedstock 2** (microalgae-based wastewater residues, referred to as “**algae residues”** in the document) and **Feedstock 6** (oily sludge). The microwave pyrolysis reactor was simulated in Aspen Plus, while the post-processing of the three fractions was modeled in Aspen HYSYS. The report also includes mass and energy balances, along with key parameter estimations, such as the process's energy efficiency.

1. INTRODUCTION

1.1 DESCRIPTION OF THE DOCUMENT AND PURSUE

This report, Deliverable 2.3, titled "Requirement List for the TRL4 Flexby System", is submitted in month 10 of the FLEXBY project. It outlines the initial requirements for the basic engineering phase of the project. In particular, the report includes:

- The general requirements defined by the consortium partners,
- The State-of-the-Art of the technological solutions applied in the process,
- The Block Flow Diagram and Process Flow Diagram (PFD), detailing the main process inputs and operating conditions,
- The datasheet with energy and mass balances of two steady-state process simulations, one for each feedstock type (algae residues and oily sludge).

This document provides the groundwork for developing the lab-scale experimental campaign of the process.

1.2 WPS AND TASKS RELATED WITH THE DELIVERABLE

This deliverable refers to Task 2.3 (General requirements for FLEXBY at lab-scale) and Task 2.4 (Detailed process simulation) included in WP2: Flexby requirements.

Below is a detailed explanation of which section of the document refers to each activity within the aforementioned tasks:

Task 2.3:

This task, led by PMI, aims to define the main process variables for the project. This analysis will include the required process unit, feedstocks requirements, heat and mass balance, instrument and tools, software for the digital twin, and all the initial requirements for the basic design for the technologies at TRL5.

Covered in sections 4, 5 and 6

A revision of the state of the art for each technology will be necessary to establish the general basic design and experimental parameters. In this phase, the coordination between the technical (US, CSIC, A4F, GALP), optimisation (IDE), microwave designer (FRIMA) and sustainability partners (GD) will be crucial in defining the preliminary requirements.

Covered in section 3

Task 2.4:

The aim of this task, led by PMI, is to perform a techno-feasibility analysis of the entire process through simulation. The simulation process, using Aspen Hysis v11, is very useful in finding and understanding all the process variables with material and heat balances for the general process.

Covered in section 5 and 6

FRIMA will also contribute to this task, performing the simulation of the microwave pyrolysis process.

Covered in section 4

IDE will support this task, suggesting optimisation inputs and outputs.

Covered in section 2

Additionally, the steady-state digital twin (DT) allows sensitivity and flexible analysis of the process to find the most sensible variable of the process. Each unit to model on the simulator will require interactions with the other members of the technical team: US, A4F, GALP, and CSIC; this feedback is important to define the upper and lower limits of design, model, and simulation and provide specific characteristics of the relative components.

Covered in section 6

2. Coordination Among Project Partners and General Requirements

PMI organized several online meetings and updates with the technical partners involved in the project, specifically:

- **FRIMA**, to discuss the requirements and design of the microwave (MW) pyrolysis reactor,
- **CSIC**, to define requirements for the oily-sludge feedstock, as well as to address the installation and hosting requirements for the MW pyrolysis reactor, as well as the scheduling of both conventional and MW algae residue pyrolysis tests,
- **US**, to define their requirements for fluid (bio-fuel) post-processing,
- **IDE**, to define the requirements for optimization,
- **A4F**, to discuss requirements of the algae residue feedstock,
- **GD**, to lay the foundations for the requirements in line with the sustainability study.

The synergies and diverse expertise of the partners enabled the pre-design of the MW pyrolysis reactor, the development of the process flow diagram and the identification of key process variables. Each meeting will be summarized focusing on the main inputs provided by the partners, which were crucial in defining the initial requirements.

FRIMA-PMI meeting

FRIMA highlighted that the MW pyrolysis reactor should operate in batch mode for several reasons, including:

- The variability of the feedstock, which requires different residence times in the unit,
- The need to carry out the process in the absence of oxygen,
- The necessity to perform multiple tests while varying humidity and other process parameters.
- More precise control over experimental parameters, higher energy efficiency, and the ability to use the same microwave system for sample drying.

FRIMA emphasized that the reactor design depends on the characteristics of the feedstock and expressed a preference for using partially dry feedstock inside the MW reactor. **PMI** requested **FRIMA** to consider a modification in the reactor design to allow operation under slight overpressure (2-3 bar) to facilitate the discharge and handling of pyrolysis gases. In response, **FRIMA** has indicated its availability to implement this design adjustment. The definition of the loading/discharging and operating times will be evaluated after the initial tests with the unit. The possibility to switch from batch to continuous mode will be considered after the testing, for the pilot scale plant. Finally, **FRIMA** highlighted that it would be beneficial to finalize the key experimental parameters in advance to ensure they are incorporated into the system design. The current design includes capabilities to measure time, temperature, microwave power, sample relative humidity at the beginning of the process, and relative pressure during the process.

CSIC-PMI meeting

CSIC will host the MW reactor at their facility and they will be responsible for the testing phase. Tests will be conducted using both the conventional and MW reactors. The main challenges are feedstock availability and unit cleaning between tests. A total of 20 to 30 tests for each feedstock will be performed, varying humidity, temperature and the external addition of char or other compounds to determine the optimal operating conditions. Each test will require between 10 to 30 g of dry feedstock. CSIC highlighted the importance of the drying phase, as high-humidity feedstock can generate odour issues. The algae residue feedstock, supplied with 70 to 90% humidity, should be at least partially dried to 10/15% before storage.

US-PMI meeting

US is responsible for pyrolysis gas and bio-liquid refining. Both **US** and **PMI** agreed that the pyrolysis gas post-processing pathway heavily depends on the composition and impurities of the gas mixture, which is not yet available at this stage of the project. As a result, the pyrolysis gas pathway may be adjusted based on the experimental results. The bio-liquid will undergo H_2-free hydrodeoxygenation to produce high-quality biofuel. However, since no experimental tests have been conducted, assumptions have been made to characterize the bio-liquid using literature data on algae residue and MW pyrolysis. Representative molecules containing all the atoms present in the feedstock have been used to characterize the three product phases. For instance, pyrrole has been chosen as a model compound for nitrogen-based molecules in the liquid phase (Ağbulut et al., 2023). These reference molecules have been selected based on existing literature studies and are listed in Tables 6.1 and 6.5. The atomic balance between reactants and products has been established while preserving, as closely as possible, the same ratio of pyrolysis gas, bio-liquid, and char reported in the literature (Zhang et al., 2016).

The biochar recovered from MW pyrolysis will be partially reintegrated into the algae residue feedstock to enhance its conductivity and partially used for activated carbon production by physical activation. MW pyrolysis tests will be conducted with different biochar quantities to determine the optimal feed mixture. Finally, **US** highlighted that the combined reforming-WGS process will not be able to fully remove CO. Therefore, given that PEMs deactivate rapidly with CO, SOFC should be considered and energetically integrated with the reforming units.

IDE-PMI meeting

IDE proposed that the variables defined in the experimental phase as discussed could later be integrated into a digital twin of the system. By developing a dynamic simulation model, these parameters can be optimized in real-time, allowing for process adjustments that enhance efficiency. This digital twin framework would facilitate process optimization, ensuring that both lab-scale and pilot-scale operations achieve maximum performance while minimizing waste and energy consumption.

A4F-PMI meeting

A4F confirmed that they can produce and supply approximately 13 kg of wet feedstock per year. Consequently, optimizing feedstock usage for determining the optimal operating conditions of MW pyrolysis is crucial to efficiently manage the limited feedstock availability.

GD-PMI meeting

GD emphasized the importance of tracking the origin of materials, as well as their lifetime and operational time, as these factors significantly affect the Life Cycle Assessment (LCA) of the overall process. Additionally, they require comprehensive process data, including both material and energy flows. **GD** also highlighted the critical role of the end-of-life phase for both the lab-scale and pilot-scale plants, as it has a substantial impact on the LCA of the entire project.

3. State-of-the-Art review

This section provides a summary and conclusions of the extensive literature review conducted for the Flexby project. The review was initiated based on the State-of-the-Art included in the Grant Agreement (GA) and further expanded to explore the operating range of key process variables and conduct a preliminary assessment, particularly for technologies not yet well documented in the literature.

The literature extensively covers the use of algae as a feedstock for bio-oil production (Ağbulut et al., 2023). However, the variability in feedstock composition and operating conditions significantly affects both yields and product distribution. In general, microwave power and operating temperature are the primary process variables studied (Du et al., 2011). The yields of gas, liquid, and solid products are strongly influenced by these parameters. In addition, bio-oil production appears to be maximized when approximately 10% of activated carbon is present in the feedstock (Zhang et al., 2016). To optimize microwave-assisted pyrolysis for minimizing energy consumption while maximizing gas and bio-liquid production, several operational parameters should be carefully controlled. Pyrolysis temperature is a critical factor, with optimal bio-oil production occurring between 450-550°C, while higher temperatures favor gas production (Mutsengerere S., et al., 2019; Ranzi et al., 2016). Microwave power and power density influence heating rates, with higher power intensities accelerating the process but requiring careful balance to avoid excessive energy consumption. The type and flow rate of the carrier gas also impact the process, as lower flow rates promote heat retention and higher bio-liquid yield, whereas increased flow rates can enhance gas production. Additionally, the use of effective microwave absorbents, such as activated carbon or biochar, improves heating efficiency and energy utilization. Proper selection of biomass particle size, helps ensuring efficient heat transfer, favoring bio-liquid formation. Finally, reactor design and stirring speed play a role, with moderate mixing enhancing heat distribution without excessive breakdown into non-condensable gases (Mutsengerere S., et al., 2019; Al-Qahtani, A.M., 2023).

The processing of pyrolysis gas involves several technologies that are well-documented in the literature and widely implemented in industrial applications. Steam methane reforming is the primary method for producing syngas from natural gas. Since pyrolysis gas can contain high concentrations of methane, its conversion is essential to minimize hydrogen losses (Bolívar Caballero et al., 2022). Optimizing operational variables in pyrolysis gas steam reforming is crucial for enhancing hydrogen production and efficiency. Some key operational variables are:

- Temperature: high temperatures generally improve conversion rates and hydrogen yields, but they also increase energy consumption and potential catalyst deactivation (Jaffar M.M., et al., 2020; Mutsengerere S., et al., 2019)
- Steam/biomass ratio influences hydrogen yield and helps in reducing coke formation on catalysts, which can lead to deactivation (Mutsengerere S., et al., 2019; Arregi, A. et al., 2018)
- Catalyst Type and Support: nickel-based catalysts are frequently used due to their effectiveness in promoting hydrogen production (Jaffar M.M., et al., 2020).

A compressor may be required to optimize the reformer unit's size and efficiency. Moreover, numerous studies (Yang, 2017) have highlighted the deactivation and poisoning of nickel-based reforming catalysts due to sulphur compounds, such as hydrogen sulfide. Given that algae often contain significant amounts of sulphur, monitoring sulphur-based compounds in the pyrolysis gas is crucial. To further enhance hydrogen production, a Water-Gas Shift (WGS) reactor can be employed. This technology is widely applied in industrial processes, particularly for increasing hydrogen yield after steam methane reforming and as a key step in ammonia production (Saeidi et al., 2017). Optimization of temperature and pressure is key to maximizing hydrogen production after gas reformation (Ikechukwu Okoji, A. et al., 2024; Babatabar M. A., et al., 2021; Youngsan, J. et al., 2020). Also, feed composition rations can lead to a higher hydrogen concentration and improve the reactor performance (Ikechukwu Okoji, A. et al., 2024). Finally, Proton Exchange Membrane (PEM) fuel cells have been chosen due to their ability to operate at low temperatures, their reliability, and high energy efficiency. The operating conditions and energy efficiency have been sourced from the literature to estimate the energy output of the fuel cells (Kazim, 2004). Since the operating pressure of the PEMs is typically between 2-4 bar, the steam methane reformer will be operated at the same pressure for engineering and economic reasons.

Regarding the bio-liquid pathway, treatment is required primarily to reduce its oxygen content. Oxygen is, in fact, one of the main elements present in the feedstock. This process is highly energy-intensive and demands large amounts of hydrogen, significantly impacting both environmental and economic aspects. Hydrodeoxygenation is an emerging technology designed to drastically lower the energy requirements of this process by using water as the main reactant (Jin et al., 2021). Optimizing this process involves adjusting conditions to maximize efficiency without relying on external hydrogen sources. For this catalyst selection support is a key factor. Also optimizing temperature, pressure, and space velocity is essential given that these parameters significantly influence the reaction kinetics and product selectivity (Zhu, Y. et al., 2015; Jin, W, et al., 2019).

The valorization of biochar is crucial for improving process efficiency. Converting waste biochar into activated carbon has been chosen as an alternative due to its use in other units, such as the microwave reactor. While the operating conditions and activation mechanisms are well understood, the application of this technology to enhance other process units has yet to be demonstrated in a relevant industrial environment (Ferrera-Lorenzo et al., 2014). The physical activation of biochar using carbon dioxide as an oxidizing agent represents an eco-friendly solution for both the valorization of waste char and the utilization of carbon dioxide. The operating conditions have been selected based on literature guidelines (Alvarez et al., 2015).

4. Initial requirements for basic engineering design

The initial requirements for basic engineering have been defined based on the detailed review of the State-of-the-Art presented in Section 3, as well as on the meetings held with each project partner. Therefore, Table 4.1 presents the operating conditions for each unit of the process system.

Six different feedstock qualities and origins were initially considered suitable for the Flexby project. The characterization of the feedstock has been conducted and detailed in Deliverable 2.1. Table 4.2 presents the proximate and ultimate analyses of the six samples.

Table 4.1. Flexby unit operation's temperatures and pressures

Operating Unit	Temperature	Pressure	Ref.
Microwave pyrolysis Reactor	700 °C	2 bar	(Du et al., 2011)
Steam Methane Reformer	900 °C	4 bar	(Bolívar Caballero et al., 2022)
Adiabatic WGS Reactor	250 °C	4 bar	(Saeidi et al., 2017)
Proton Exchange Membrane	50 – 80 °C	1.5 – 3 bar	(Kazim, 2004)
Hydrodeoxygenation Reactor	250 °C	16 bar	(Jin et al., 2021)
Physical activation of biochar	800 °C	Atmospheric	(Alvarez et al., 2015)

Table 4.2. Proximate and Ultimate analysis of the feedstocks

Biomass waste	**Humidity (%)**	**VM (%) [a]**	**Ash (%) [a]**	**C (%) [a]**	**H (%) [a]**	**N (%) [a]**	**S (%) [a]**	**O (%) [a, b]**
Feedstock1	85.9	62.7*	24.43	40.56	5.80	5.79	0.35	23.07
Feedstock2	84.3	62.98**	22.26 34.00**	41.73	6.19	4.10	0.25	25.47
Feedstock3	79.2	36.19	60.22	18.78	2.36	3.58	1.06	14.00
Feedstock4	86.0	51.25	41.07	28.58	3.72	5.47	1.00	20.16
Feedstock5	84.5	72.29	22.56	44.20	6.18	5.50	0.55	21.01
Feedstock6	75.9	79.80	13.35	54.31	8.45	5.88	0.38	17.63

[a] dry basis
[b] calculated by difference
* Due to the lack of Feedstock1, its volatile matter content was estimated from the pyrolysis curve.
** Results of sample Feedstock2 received in October 2024, equivalent to Feedstock2 received in July 2024.

4.1 Block Flow Diagram and required process units

The block flow diagram of the Flexby project is shown in Figure 4.1. As illustrated, the feedstock is introduced into the MW pyrolysis reactor without prior drying. The resulting three fractions are then collected and processed separately.

The MW reactor operates at a maximum power of 3 kW and has a capacity of 2 kg of wet feedstock. The pre-design of the MW reactor, provided by FRIMA, is shown in Figure 4.2. The operation phase of the unit is divided into 2 stages. The first stage is the drying process, hot air enters from the top and vapor is recovered to reduce the humidity of the feedstock. In the second stage, nitrogen is introduced (also from the top, at flow rates between 0.1 to 1 L/min) to ensure an oxygen-free environment during the pyrolysis process. The maximum temperature of the product reaches approximately 700°C, in line with literature data. The system is designed to withstand higher pressures of up to 3 bar.

The H_2-free hydrodeoxygenation is a batch process working at approximately 150 bar and 250-300 °C, with a residence time ranging from 1 to 12 hours. The experimental tests of this unit will require 25 to 50 ml of the bio-liquid mixture, mixed with 40 mL of water.

The pyrolysis gas must be post-processed to obtain H_2-rich gas. The preliminary process scheme consists of:

- A separator to remove water from the gas mixture,
- A reforming unit, which enables the nearly complete conversion of methane into hydrogen, carbon monoxide, and carbon dioxide,
- A water-gas shift (WGS) reactor, where water is added before the reaction to enhance hydrogen production.

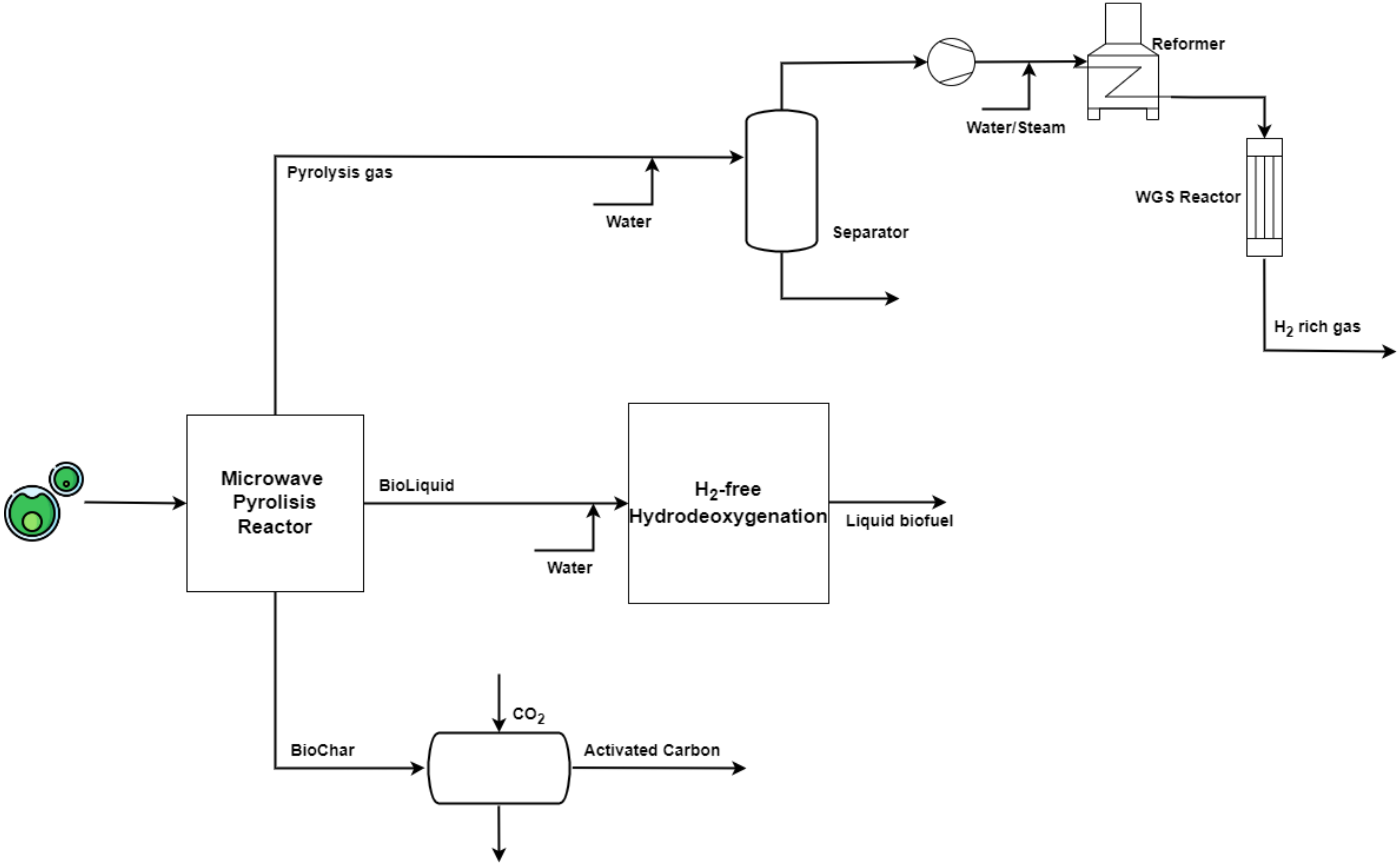

Figure 4.1. Block Flow Diagram of the Flexby process.

Pressures and temperatures have been selected based on literature data and industrial standards (Bolívar Caballero et al., 2022; Saeidi et al., 2017). However, since the primary objective is hydrogen production for electric energy generation in a Proton Exchange Membrane (PEM) fuel cell, the reformer pressure is limited to 4 bar, aligning with the operating pressure required by PEM fuel cells (Askaripour, 2019).

The lab-scale experimental tests will be conducted in batch mode. However, the pilot-scale plant, which will be installed at **US** facilities, will operate continuously. To ensure a stable flow of gas and liquid for post-processing, buffer units will be installed between the MW pyrolysis reactor and the rest of the process.

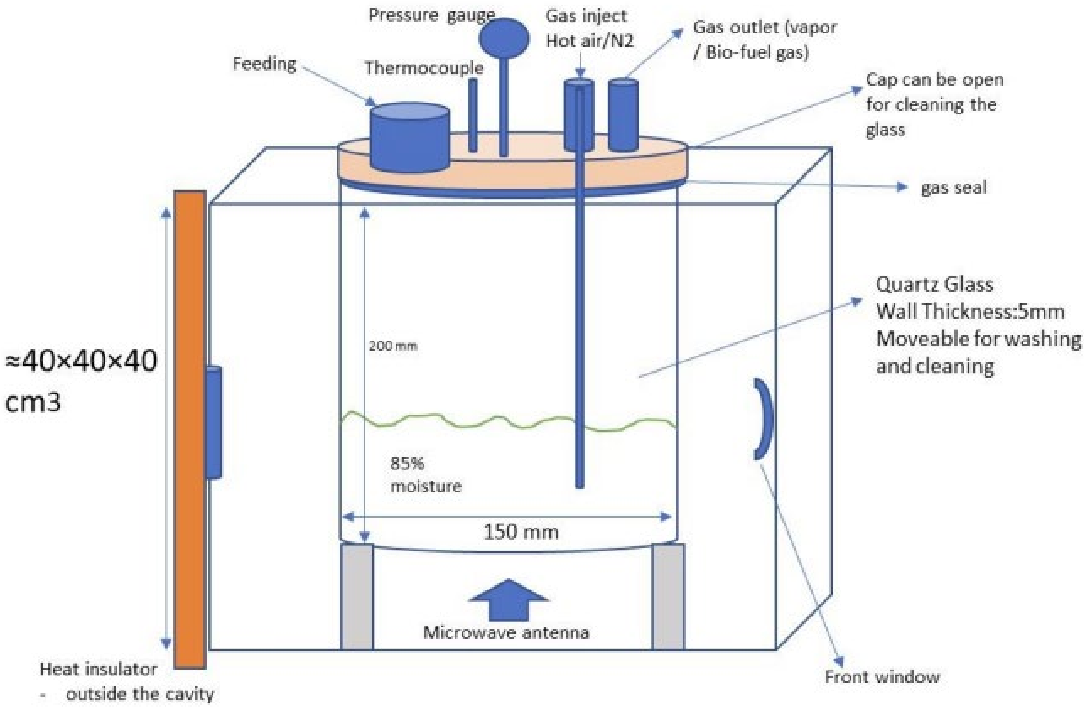

Figure 4.2. Pre-design of the Microwave Pyrolysis Reactor.

5. Simulation and techno-feasibility analysis of the process

In this section, the two steady-state simulations of the Flexby process are presented, using **Feedstock 2** (Table 4.2) to represent algae residue feedstock and **Feedstock 6** (Table 4.2) to represent oily sludge from the dairy industry feedstock, respectively. The characterization of the feedstocks is detailed in Deliverable 2.1 of this project.

This section begins with the presentation of the process flow diagram for the simulation, which remains consistent regardless of the feedstock chosen. This is followed by the definition of input variables, output variables, and assumptions. Finally, datasheets for both material and energy streams are provided for each simulation. At this project stage, pressure drops in heat exchangers have been neglected.

The following tools were employed to support the simulations explained below:

- Aspen PLUS V14 and Aspen HYSYS V14 were used to simulate the process. Aspen PLUS V14 has been employed to model the MW pyrolysis reactor in the absence of experimental data (Corbetta et al., 2016).
- Microsoft Excel was used to solve the mass balance between feedstocks and MW pyrolysis products.
- Additionally, Aveva Dynamic Simulator will be used to perform a dynamic simulation of the process. This tool will help analyze the system’s response to variations in feed conditions and operational fluctuations.

5.1 Process Flow Diagram of Flexby process

Figure 5.1 illustrates the simulation of the microwave pyrolysis reactor in Aspen Plus V14. As shown, the feedstock (FEED in Figure 5.1) enters the MW reactor, where pyrolysis takes place. The resulting product stream (PYR-PROD in Figure 5.1) is then directed to a virtual component splitter, which separates it into three fractions: pyrolysis gas (PYROGAS in Figure 5.1), bio-liquid (BIOLIQ in Figure 5.1), and residual solid (SOLID in Figure 5.1),.

As previously mentioned, the composition of the pyrolysis products has been determined by solving the atomic balance of the reactor. The process simulation has been utilized to calculate the enthalpy difference between the feedstock and the resulting products.

The Non-Conventional Component Tool has been applied to estimate the specific enthalpy of the feedstock based on the proximate and ultimate analysis provided in Deliverable 2.1.

The three material streams are then imported into Aspen HYSYS V14 for post-processing.

Table 5.1 presents the input parameters for the simulation of the MW pyrolysis reactor.

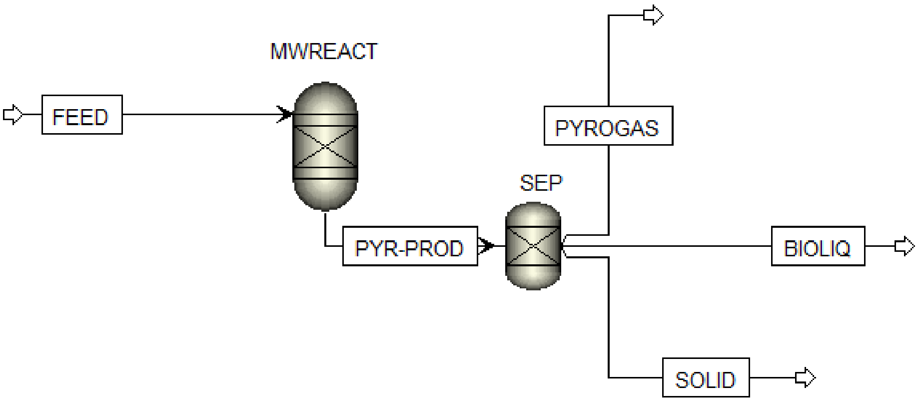

Figure 5.1. Simulation of the MW pyrolysis reactor in Aspen Plus V14

Table 5.1. Input parameters for Aspen Plus simulation

	Temperature	Pressure
Feedstock	25 °C	2 bar
Pyrolysis Product	700 °C	2 bar

Concerning the pyrolysis gas pathway, Figure 5.2 and Figure 5.3 illustrate the simulation implemented in Aspen HYSYS V14, while Figure 5.4 presents the Process Flow Diagram (PFD) along with the material and energy stream names.

For the process description, please refer to the stream numbers shown in Figure 5.4.

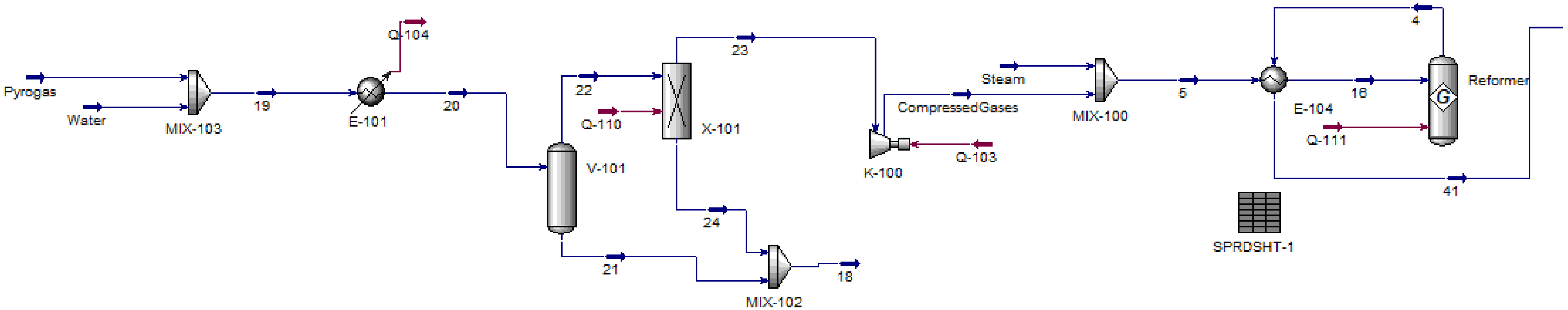

Figure 5.2. First section of the pyrolysis gas post-processing simulation in Aspen HYSYS V14

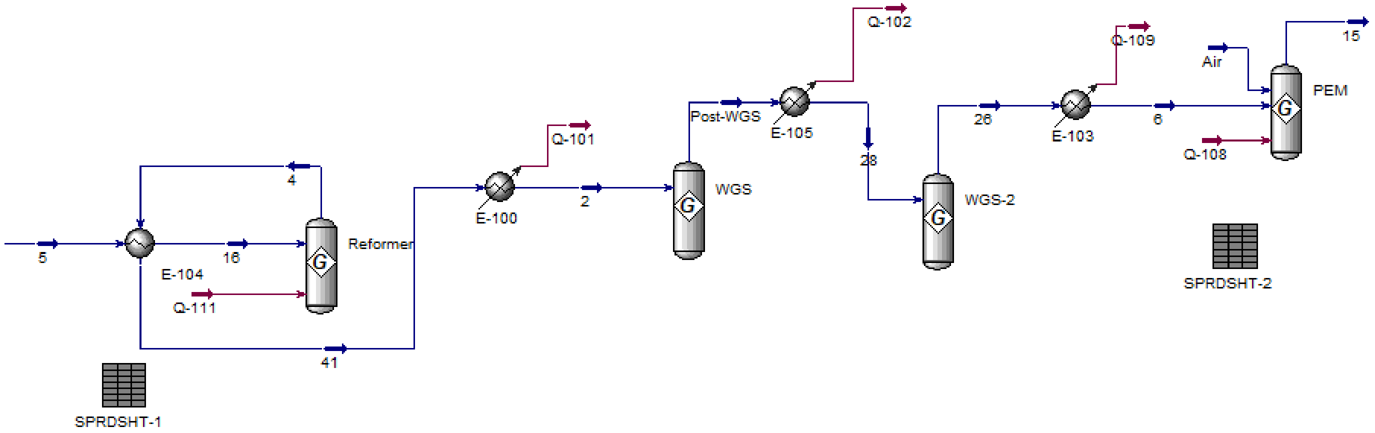

Figure 5.3. Second section of the pyrolysis gas post-processing simulation in Aspen HYSYS V14

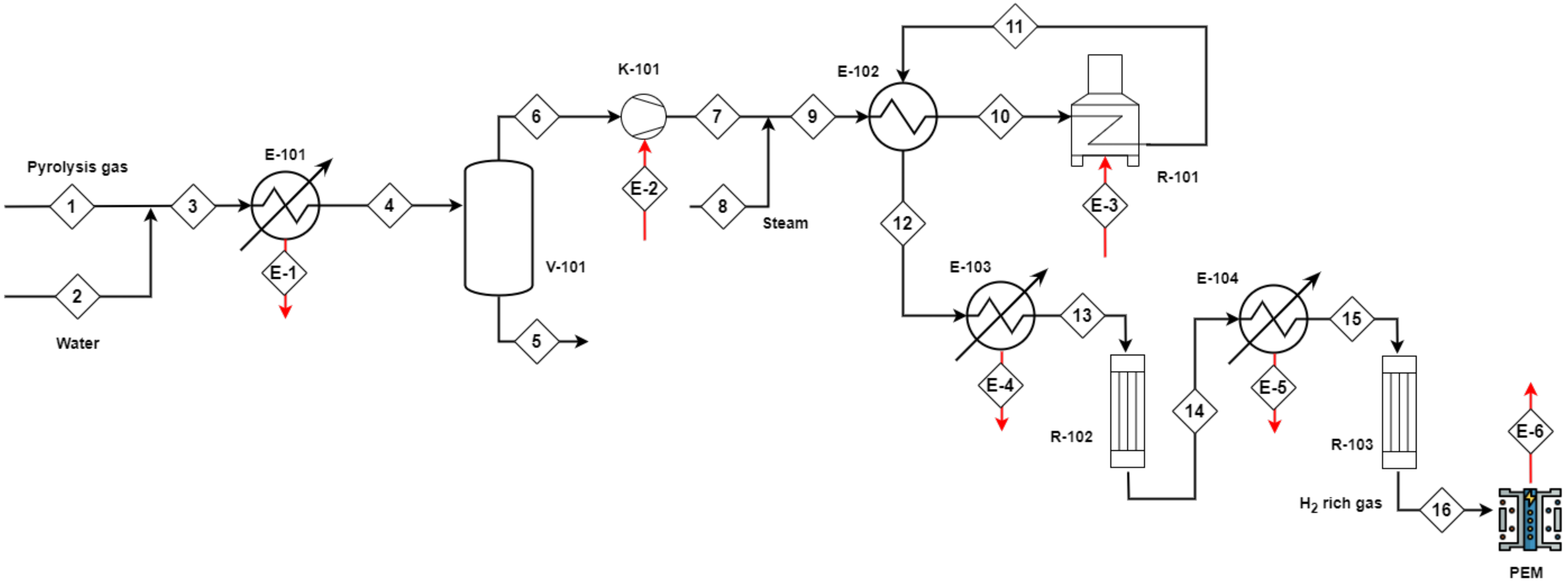

Figure 5.4. Process Flow Diagram (PFD) of pyrolysis gas post-processing

The pyrolysis gas (stream 1) is initially mixed with water (stream 2) to reduce its temperature from 700 °C to 70 °C. The stream is then further cooled to 30 °C in heat exchanger E-101, allowing for the separation of water and ammonia (stream 5) in separator V-101. The resulting gas stream (stream 6) is compressed in compressor K-101 to reach the operating pressure of the reformer, equal to 4 bar (R-101). Before entering the reformer, steam (stream 8) is added, and the mixture passes through a process-to-process heat exchanger (E-102), which utilizes the heat from the reformer product (stream 11) to preheat the inlet mixture (stream 10). The reformed gas (stream 11) is subsequently cooled to 250 °C using water (heat exchanger E-103) to reach the required temperature for the first adiabatic water-gas shift (WGS) reactor (R-102). The gas product (stream 14) is further cooled to 250 °C before entering the second adiabatic WGS reactor (R-103). Finally, the hydrogen-rich stream (stream 16) is directed to a PEM fuel cell for electric energy generation.

Table 5.2 presents the input stream temperatures and pressures. It has been assumed that the reactors operate at thermodynamic equilibrium, as the reactions involved are thermodynamically limited. The mass flow rates of streams 2 and 8 have been determined by setting, respectively, the temperature of stream 3 and a hydrogen-to-carbon ratio of 3 (Bolívar Caballero et al., 2022). The Soave-Redlich-Kwong (SRK) equation of state has been chosen to model the mixture behavior.

Table 5.2. Input parameters for pyrolysis gas post-processing Aspen HYSYS simulation

Stream number	Temperature [°C]	Pressure [bar]
1	700	2
2	30	2
3	70	-
4	30	-
7	-	4
10	500	-
13	250	-
15	250	-

Figure 5.5 illustrates the simulation of the bio-liquid refining in Aspen HYSYS, while Figure 5.6 shows the process flow diagram of the process. For the process description, refer to the stream numbers shown in Figure 5.6.

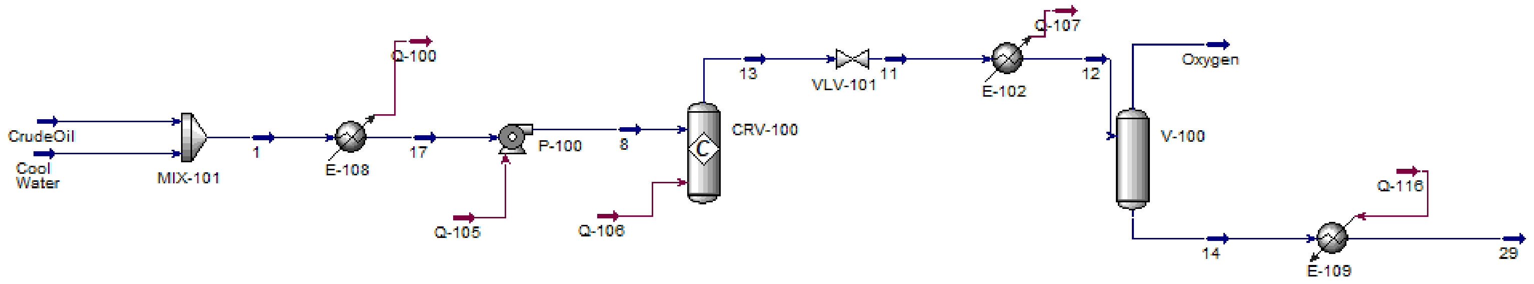

Figure 5.5. Bio-liquid post-processing simulation in Aspen HYSYS V14

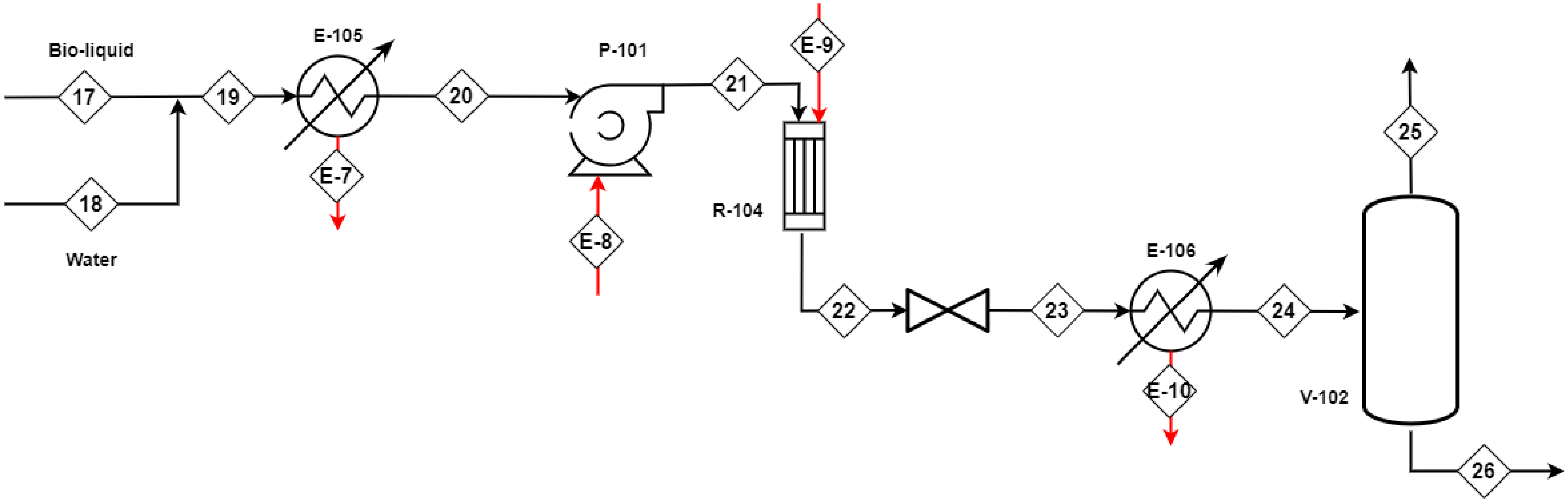

Figure 5.6. Process Flow Diagram of bio-liquid refining

The bio-liquid recovered from the MW pyrolysis reactor (stream 17) is first mixed with water (stream 18) to cool down the mixture. The resulting stream (19) is further cooled to 60 °C in heat exchanger E-105 with cooling water. The condensed stream (20) is then pressurized to 16 bar by pump P-101 to reach the hydrodeoxygenation (HDO) operating pressure, producing stream 21. The HDO product (stream 22) is subsequently flashed (via a valve and heat exchanger E-106) to separate the gas phase (stream 25) from the refined bio-oil (stream 26). Table 5.2 presents the fixed input parameters used in the simulation to model the process system.

Table 5.3. Input parameters for bio-liquid refining Aspen HYSYS simulation

Stream number	Temperature [°C]	Pressure [bar]
17	700	2
18	30	2
20	60	-
21	-	16
22	250	-
23	-	2
24	50	-

Regarding activated carbon production, it has been assumed that 50% of the initial char mass volatilizes (Goel et al., 2021). The stoichiometry of the reactants and the operating conditions will be determined through subsequent experimental tests.

6. Datasheet, energy and mass balances

The following section is divided into two subsections, each dedicated to one of the feedstock types considered in the project. The first subsection presents the datasheet and the energy and mass balance for the process starting from Feedstock 2, which represents the algae residue feedstock. The same structure is then applied to Feedstock 6, representing the oily sludge feedstock. The next tables refer to Figure 5.4 and Figure 5.6 for the stream numbers. The feedstock mass basis for the simulation is 100 kg/h on a wet basis.

A critical comparison of the two simulations, along with the identification of the main process variables, is conducted in the subsequent subsection.

6.1 Algae residue feedstock (Feedstock 2)

Table 6.1 presents the three fractions obtained from the microwave pyrolysis reactor. The remaining portion, amounting to 84.2 kg/h, consists of vapor. As illustrated, due to the high moisture content of the wet feedstock (Table 4.2), a significant portion of the feedstock is converted into water. These mixtures are then imported into Aspen HYSYS for post-processing.

Table 6.1. Products of the microwave pyrolysis of Feedstock 2

Pyrolysis Gas		Bio Liquid		Solid	
Component	Mass Flow kg/h	Component	Mass Flow kg/h	Component	Mass Flow kg/h
Hydrogen	0.1109	Pyrrole	1.3863	Char	2.1042
CO_2	1.5406	$C_8H_{14}O_4$	5.9794	Ash	3.5300
CO	0.5311	Toluene	0.0537		
Methane	0.1984				
Ammonia	0.3502				
Total	2.7311	Total	7.4194	Total	5.6442

Table 6.2 presents the datasheet for the post-processing of pyrolysis gas. As shown, the post-processing results in the production of approximately 0.22 kg/h of hydrogen, starting from 100 kg/h of wet feedstock. As previously mentioned, assuming a PEM fuel cell efficiency of 50%, the recovered energy amounts to 3.66 kW.

Table 6.2. Pyrolysis gas post-processing datasheet (see Figure 5.4 for stream numbers, Feedstock 2)

Stream number	**1**	**2**	**3**	**4**	**5**	**6**
Vapor Fraction	1	0	0.422	0.285	0	1
Temperature [°C]	700	30	70	30	30	30
Pressure [bar]	1.01	1.01	1.01	1.01	1.01	1.01
Molar Flow [kmol/h]	0.14	0.33	0.47	0.47	0.35	0.12
Mass Flow [kg/h]	2.73	5.90	8.63	8.63	6.25	2.38
Molar fraction						
Hydrogen	0.39	0.00	0.12	0.12	0.00	0.45
CO_2	0.25	0.00	0.07	0.07	0.00	0.29

CO	0.13	0.00	0.04	0.04	0.00	0.16
Methane	0.09	0.00	0.03	0.03	0.00	0.10
Ammonia	0.14	0.00	0.04	0.04	0.94	0.00
Water	0.00	1.00	0.70	0.70	0.06	0.00
Stream number	**7**	**8**	**9**	**10**	**11**	**12**
Vapor Fraction	1	1	1	1	1	1
Temperature [°C]	195	250	208	500	900	642
Pressure [bar]	4.00	4.00	4.00	4.00	4.00	4.00
Molar Flow [kmol/h]	0.12	0.04	0.16	0.16	0.18	0.18
Mass Flow [kg/h]	2.38	0.67	3.05	3.05	3.05	3.05
Molar fraction						
Hydrogen	0.45	0.00	0.35	0.35	0.42	0.42
CO_2	0.29	0.00	0.22	0.22	0.11	0.11
CO	0.16	0.00	0.12	0.12	0.26	0.26
Methane	0.10	0.00	0.08	0.08	0.00	0.00
Ammonia	0.00	0.00	0.00	0.00	0.00	0.00
Water	0.00	1.00	0.23	0.23	0.22	0.22
Stream number	**13**	**14**	**15**	**16**		
Vapor Fraction	1	1	1	1		
Temperature [°C]	250	406	250	299		
Pressure [bar]	4.00	4.00	4.00	4.00		
Molar Flow [kmol/h]	0.18	0.18	0.18	0.18		
Mass Flow [kg/h]	3.05	3.05	3.05	3.05		
Molar fraction						
Hydrogen	0.42	0.55	0.55	0.59		
CO_2	0.11	0.24	0.24	0.28		
CO	0.26	0.12	0.12	0.08		
Methane	0.00	0.00	0.00	0.00		
Ammonia	0.00	0.00	0.00	0.00		
Water	0.22	0.09	0.09	0.05		

Table 6.3 presents the datasheet for bio-liquid refining. The presence of nitrogen-based molecules needs to be confirmed through experimental tests. Additionally, the presence of nitrogen- or sulfur-based compounds could pose a potential risk for the application of a Solid Oxide Electrolysis Cell (SOEC). The refining of crude bio-oil derived from the microwave pyrolysis process results in the production of 3.62 kg/h of octane. Assuming a fuel cell efficiency of 50% and a lower heating value (LHV) of 44.4 MJ/kg, the estimated energy production is approximately 22.3 kW.

Table 6.3. Bio-liquid refining datasheet (see Figure 5.6 for stream numbers, Feedstock 2)

Stream number	**17**	**18**	**19**	**20**	**21**
Vapor Fraction	1	0	1	0	0
Temperature [°C]	700	30	473	60	60
Pressure [bar]	1.01	1.01	1.01	1.01	16.00
Molar Flow [kmol/h]	0.06	0.07	0.12	0.12	0.12
Mass Flow [kg/h]	7.42	1.24	8.66	8.66	8.66
Molar fraction					
Pyrrole	0.37	0.00	0.17	0.17	0.17
Toluene	0.01	0.00	0.00	0.00	0.00
$C_8H_{14}O_4$	0.62	0.00	0.28	0.28	0.28
Oxygen	0.00	0.00	0.00	0.00	0.00
C_8H_{14}	0.00	0.00	0.00	0.00	0.00
Water	0.00	1.00	0.55	0.55	0.55
Stream number	**22**	**23**	**24**	**25**	**26**
Vapor Fraction	1	1	0.679	1	0
Temperature [°C]	250	245	50	50	50
Pressure [bar]	16.00	2.00	2.00	2.00	2.00
Molar Flow [kmol/h]	0.16	0.16	0.16	0.11	0.05
Mass Flow [kg/h]	8.66	8.66	8.66	3.74	4.92
Molar fraction					
Pyrrole	0.13	0.13	0.13	0.02	0.36

Toluene	0.00	0.00	0.00	0.00	0.01
$C_8H_{14}O_4$	0.00	0.00	0.00	0.00	0.00
Oxygen	0.65	0.65	0.65	0.95	0.00
C8H14	0.22	0.22	0.22	0.02	0.62
Water	0.00	0.00	0.00	0.00	0.00

Finally, assuming a volatilization of 50% of the initial char, the production of activated carbon is estimated to be approximately 1.05 kg/h.

Table 6.4 presents the energy streams required for pyrolysis gas post-processing and bio-liquid refining. It is important to note that E-2 and E-8 represent electric energy streams, while negative values indicate energy leaving the system (due to cooling). Additionally, the power demand for the microwave pyrolysis process is estimated to be approximately 37 kW, assuming that the feedstock is partially dried with a moisture content of 10%.

Table 6.4. Energy streams of the process (see Figures 5.4 and 5.6 for stream numbers, Feedstock 2)

Energy stream	**E-1**	**E-2**	**E-3**	**E-4**	**E-5**
Heat Flow [kW]	-1.16	0.09	1.64	-0.68	-0.27
Energy stream	**E-6**	**E-7**	**E-8**	**E-9**	**E-10**
Heat Flow [kW]	3.66	-4.06	0.01	14.04	-1.31

6.2 Oily-sludge feedstock (Feedstock 6)

Table 6.5 presents the three fractions obtained from the microwave pyrolysis reactor with the oily-sludge feedstock (Feedstock 6, Table 4.2). The amount of vapor is equal to 75.9 kg/h. These mixtures are then imported into Aspen HYSYS for post-processing.

Table 6.5. Products of the microwave pyrolysis of Feedstock 6

Pyrolysis Gas		Bio Liquid		Solid	
Component	Mass Flow kg/h	Component	Mass Flow kg/h	Component	Mass Flow kg/h
Hydrogen	0.1117	Pyrrole	3.0518	Char	3.8523
CO_2	0.6655	$C_8H_{14}O_4$	6.3533	Ash	3.3100
CO	1.8352	Benzene	0.6301		
Methane	0.8470	C_6H_{14}	2.6689		
Ammonia	0.7752				
Total	4.2347	Total	12.7041	Total	7.1623

Table 6.6 presents the datasheet for the post-processing of pyrolysis gas. As shown, the post-processing results in the production of approximately 0.59 kg/h of hydrogen, starting from 100 kg/h of wet feedstock. As previously mentioned, assuming a PEM fuel cell efficiency of 50%, the recovered energy amounts to 9.82 kW.

Table 6.6. Pyrolysis gas post-processing datasheet (see Figure 5.4 for stream numbers, Feedstock 6)

Stream number	**1**	**2**	**3**	**4**	**5**	**6**
Vapor Fraction	1	0	0.333	0.217	0	1
Temperature [°C]	700	30	70	30	30	30
Pressure [bar]	1.01	1.01	1.01	1.01	1.01	1.01
Molar Flow [kmol/h]	0.24	0.72	0.96	0.96	0.77	0.18
Mass Flow [kg/h]	4.24	13.00	17.24	17.24	13.86	3.38
Molar fraction						
Hydrogen	0.23	0.00	0.06	0.06	0.00	0.29
CO_2	0.06	0.00	0.02	0.02	0.00	0.08
CO	0.27	0.00	0.07	0.07	0.00	0.35

Methane	0.22	0.00	0.05	0.05	0.00	0.28
Ammonia	0.21	0.00	0.05	0.05	0.07	0.00
Water	0.00	1.00	0.75	0.75	0.93	0.00

Stream number	**7**	**8**	**9**	**10**	**11**	**12**
Vapor Fraction	1	1	1	1	1	1
Temperature [°C]	198	250	221	500	900	671
Pressure [bar]	4.00	4.00	4.00	4.00	4.00	4.00
Molar Flow [kmol/h]	0.18	0.15	0.34	0.34	0.44	0.44
Mass Flow [kg/h]	3.38	2.79	6.17	6.17	6.17	6.17
Molar fraction						
Hydrogen	0.29	0.00	0.16	0.16	0.50	0.50
CO2	0.08	0.00	0.04	0.04	0.07	0.07
CO	0.35	0.00	0.19	0.19	0.22	0.22
Methane	0.28	0.00	0.15	0.15	0.00	0.00
Ammonia	0.00	0.00	0.00	0.00	0.00	0.00
Water	0.00	1.00	0.46	0.46	0.20	0.20

Stream number	**13**	**14**	**15**	**16**
Vapor Fraction	1	1	1	1
Temperature [°C]	250	393	250	293
Pressure [bar]	4.00	4.00	4.00	4.00
Molar Flow [kmol/h]	0.44	0.44	0.44	0.44
Mass Flow [kg/h]	6.17	6.17	6.17	6.17
Molar fraction				
Hydrogen	0.50	0.62	0.62	0.66
CO_2	0.07	0.19	0.19	0.22
CO	0.22	0.10	0.10	0.07
Methane	0.00	0.00	0.00	0.00
Ammonia	0.00	0.00	0.00	0.00
Water	0.20	0.08	0.08	0.04

Table 6.7 presents the datasheet for bio-liquid refining starting from Feedstock 6. The presence of nitrogen-based molecules needs to be confirmed through experimental tests. Additionally, the presence of nitrogen- or sulfur-based compounds could pose a potential risk for the application of a Solid Oxide Electrolysis Cell (SOEC). The refining of crude bio-oil derived from the microwave pyrolysis process results in the production of 3.97 kg/h of octane and 1.94 kg/h of hexane. Assuming a fuel cell efficiency of 50% and a lower heating value (LHV) respectively of 44.4 and 47.2 MJ/kg, the estimated energy production is approximately 37.3 kW.

Table 6.7. Bio-liquid refining datasheet (see Figure 5.6 for stream numbers, Feedstock 6)

Stream number	**17**	**18**	**19**	**20**	**21**
Vapor Fraction	1.00	0.00	1.00	0.00	0.00
Temperature [°C]	700	30	567	60	60
Pressure [bar]	1.01	1.01	1.01	1.01	16.00
Molar Flow [kmol/h]	0.12	0.07	0.19	0.19	0.19
Mass Flow [kg/h]	12.70	1.31	14.02	14.02	14.02
Molar fraction					
Pyrrole	0.38	0.00	0.23	0.23	0.23
Toluene	0.00	0.00	0.00	0.00	0.00
Benzene	0.07	0.00	0.04	0.04	0.04
$C_8H_{14}O_4$	0.30	0.00	0.19	0.19	0.19
Oxygen	0.00	0.00	0.00	0.00	0.00
C_8H_{14}	0.00	0.00	0.00	0.00	0.00
C_6H_{14}	0.26	0.00	0.16	0.16	0.16
Water	0.00	1.00	0.38	0.38	0.38
Stream number	**22**	**23**	**24**	**25**	**26**
Vapor Fraction	1.00	1.00	0.53	1.00	0.00
Temperature [°C]	250	243	50	50	50
Pressure [bar]	16.00	2.00	2.00	2.00	2.00
Molar Flow [kmol/h]	0.23	0.23	0.23	0.12	0.11
Mass Flow [kg/h]	14.02	14.02	14.02	4.70	9.32
Molar fraction					

Pyrrole	0.20	0.20	0.20	0.02	0.40
Toluene	0.00	0.00	0.00	0.00	0.00
Benzene	0.04	0.04	0.04	0.01	0.06
C8H14O4	0.00	0.00	0.00	0.00	0.00
Oxygen	0.47	0.47	0.47	0.89	0.00
C8H14	0.16	0.16	0.16	0.01	0.32
C6H14	0.13	0.13	0.13	0.07	0.21
Water	0.00	0.00	0.00	0.00	0.00

Concerning the valorization of char, assuming a volatilization of 50% of the solid residue, the production of activated carbon is estimated to be approximately 1.92 kg/h.

Table 6.8 presents the energy streams required for pyrolysis gas post-processing and bio-liquid refining. It is important to note that E-2 and E-8 represent electric energy streams, while negative values indicate energy leaving the system (due to cooling). Additionally, the power demand for the microwave pyrolysis process is estimated to be approximately 88 kW, assuming that the feedstock is partially dried with a moisture content of 10%.

Table 6.8. Energy streams of the process (see Figures 5.4 and 5.6 for stream numbers, Feedstock 6)

Energy stream	**E-1**	**E-2**	**E-3**	**E-4**	**E-5**
Heat Flow [kW]	-2.10	0.13	4.67	-1.71	-0.85
Energy stream	**E-6**	**E-7**	**E-8**	**E-9**	**E-10**
Heat Flow [kW]	9.82	-7.07	0.01	15.94	-2.38

6.3 Comparison between Feedstock 2 and Feedstock 6 and critical parameters definition

Regarding the microwave pyrolysis reactor, it is evident that moisture content is a key variable, as it strongly impacts the gas and liquid yields on a wet basis. The power demand of the MW reactor does not seem to significantly depend on the feedstock quality, since the percentage increase in power is almost equal to the percentage increase in mass flow on a dry basis. Additionally, the yields on a dry basis are quite similar between the two feedstocks. However, the higher oxygen content in Feedstock 2, coupled with its lower carbon and hydrogen content, leads to a higher production of carbon dioxide or oxygen-based compounds, which results in a lower energy efficiency of the process.

Concerning the pyrolysis gas and bio-liquid post-processing, the identification of impurities in the feedstocks is crucial to prevent catalyst poisoning in the steam reforming or hydrodeoxygenation sections. Additionally, residence times and operating conditions during the reactive stage play a fundamental role in maximizing the energy efficiency of the process. As a preliminary estimation, the energy efficiency of the system (calculated as the ratio between the energy required by the process and the energy recovered from fuel cells) is approximately 46% for Feedstock 2 and 39.6% for Feedstock 6.

7. Conclusions

The definition of the initial requirements and process variables was essential to establishing the groundwork for constructing the microwave pyrolysis reactor and conducting lab-scale experimental tests on both pyrolysis gas post-processing and bio-liquid refining.

First, meetings with technical partners identified critical challenges related to feedstock moisture content and the operating conditions of the microwave pyrolysis reactor, which were subsequently resolved. Once the initial requirements for each process partner were defined, a Block Flow Diagram of the entire process was developed and shared with the consortium partners. In parallel, determining the quantity of feedstock required by CSIC and US was crucial for managing feedstock availability and defining the operating conditions and capacity of the microwave pyrolysis reactor.

Following this, two feedstocks were selected for steady-state process simulations: Feedstock 2 (algae residue feedstock) and Feedstock 6 (oily sludge feedstock), chosen based on recommendations from Deliverable 2.1. The simulations were conducted using Aspen PLUS for microwave pyrolysis and Aspen HYSYS for post-processing modeling, with mass and energy balances reported in this document. This study enabled the definition of all process parameters and the identification of key critical variables within the system. In particular, monitoring impurities, especially nitrogen- and sulfur-based molecules, is crucial to prevent catalyst poisoning during steam methane reforming, the WGS reaction, and the hydrodeoxygenation reaction. Finally, the energy efficiencies were estimated to evaluate the preliminary solution’s economic and environmental impact.

8. REFERENCES

Ü. Ağbulut, R. Sirohi, E. Lichtfouse, W.-H. Chen, C. Len, P.L. Show, A.T. Le, X.P. Nguyen, A.T. Hoang, 2023. Microalgae bio-oil production by pyrolysis and hydrothermal liquefaction: Mechanism and characteristics. *Bioresource Technology* 376, 128860.

A.M. Al-Qahtani, 2023. A comprehensive review in microwave pyrolysis of biomass, syngas production and utilization. *Energies* 16(19), 6876.

J. Alvarez, G. Lopez, M. Amutio, J. Bilbao, M. Olazar, 2015. Physical Activation of Rice Husk Pyrolysis Char for the Production of High Surface Area Activated Carbons. *Ind. Eng. Chem. Res.* 54, 7241–7250.

A. Arregi, G. Lopez, M. Amutio, M. Artetxe, I. Barbarias, J. Bilbao, M. Olazar, 2018. Role of operating conditions in the catalyst deactivation in the in-line steam reforming of volatiles from biomass fast pyrolysis. *Fuel* 216, 233–244.

H. Askaripour, 2019. Effect of operating conditions on the performance of a PEM fuel cell. *International Journal of Heat and Mass Transfer* 144, 118705.

J.J. Bolívar Caballero, I.N. Zaini, W. Yang, 2022. Reforming processes for syngas production: A mini-review on the current status, challenges, and prospects for biomass conversion to fuels. *Applications in Energy and Combustion Science* 10, 100064.

M. Corbetta, I.E. Grossmann, F. Manenti, 2016. Process simulator-based optimization of biorefinery downstream processes under the Generalized Disjunctive Programming framework. *Computers and Chemical Engineering 88*, 73–85

Z. Du, Y. Li, X. Wang, Y. Wan, Q. Chen, C. Wang, X. Lin, Y. Liu, P. Chen, R. Ruan, 2011. Microwave-assisted pyrolysis of microalgae for biofuel production. *Bioresource Technology* 102, 4890–4896.

N. Ferrera-Lorenzo, E. Fuente, I. Suárez-Ruiz, B. Ruiz, 2014. KOH activated carbon from conventional and microwave heating system of a macroalgae waste from the Agar–Agar industry. *Fuel Processing Technology* 121, 25–31.

C. Goel, S. Mohan, P. Dinesha, 2021. CO2 capture by adsorption on biomass-derived activated char: A review. *Science of The Total Environment* 798, 149296.

M.M. Jaffar, M.A. Nahil, P.T. Williams, 2020. Synthetic natural gas production from the three-stage (i) pyrolysis (ii) catalytic steam reforming (iii) catalytic hydrogenation of waste biomass. *Fuel Processing Technology* 208, 106515.

W. Jin, L. Pastor-Pérez, J.J. Villora-Picó, M.M. Pastor-Blas, J.A. Odriozola, A. Sepúlveda-Escribano, T.R. Reina, 2021. In-situ HDO of guaiacol over nitrogen-doped activated carbon supported nickel nanoparticles. *Applied Catalysis A: General* 620, 118033.

A. Kazim, 2004. Exergy analysis of a PEM fuel cell at variable operating conditions. *Energy Conversion and Management* 45, 1949–1961.

S. Mutsengerere, C.H. Chihobo, D. Musademba, I. Nhapi, 2019. A review of operating parameters affecting bio-oil yield in microwave pyrolysis of lignocellulosic biomass. *Renewable and Sustainable Energy Reviews* 104, 328–336.

E. Ranzi, T. Faravelli, F. Manenti, 2016. Pyrolysis, Gasification, and Combustion of Solid Fuels. *Advances in Chemical Engineering* 49, 1–94

S. Saeidi, F. Fazlollahi, S. Najari, D. Iranshahi, J.J. Klemeš, L.L. Baxter, 2017. Hydrogen production: Perspectives, separation with special emphasis on kinetics of WGS reaction: A state-of-the-art review. *Journal of Industrial and Engineering Chemistry* 49, 1–25.

C. Yang, R. Li, B. Zhang, Q. Qiu, B. Wang, H. Yang, Y. Ding, C. Wang, 2019. Pyrolysis of microalgae: A critical review. *Fuel Processing Technology* 186, 53–72.

X. Yang, 2017. An experimental investigation on the deactivation and regeneration of a steam reforming catalyst. *Renewable Energy* 112, 17–24.

R. Zhang, L. Li, D. Tong, C. Hu, 2016. Microwave-enhanced pyrolysis of natural algae from water blooms. *Bioresource Technology* 212, 311–317.

Y. Zhu, Y. Zhang, Y. Dan, Y. Yuan, L. Zhang, W. Li, D. Li, 2015. Optimization of reaction variables and macrokinetics for the hydrodeoxygenation of full range low-temperature coal tar. *Reaction Kinetics, Mechanisms and Catalysis* 116, 433–450.